

# Compound heterozygous *NOTCH1* mutations underlie impaired cardiogenesis in a patient with hypoplastic left heart syndrome

Jeanne L. Theis<sup>1</sup> · Sybil C. L. Hrstka<sup>4,5</sup> · Jared M. Evans<sup>6</sup> · Megan M. O’Byrne<sup>6</sup> · Mariza de Andrade<sup>6</sup> · Patrick W. O’Leary<sup>2,3</sup> · Timothy J. Nelson<sup>2,4,5</sup> · Timothy M. Olson<sup>1,2,3</sup>

Received: 7 May 2015 / Accepted: 2 July 2015 / Published online: 12 July 2015  
© Springer-Verlag Berlin Heidelberg 2015

**Abstract** Hypoplastic left heart syndrome (HLHS) is a severe congenital heart defect (CHD) that necessitates staged, single ventricle surgical palliation. An increased frequency of bicuspid aortic valve (BAV) has been observed among relatives. We postulated number of mutant alleles as a molecular basis for variable CHD expression in an extended family comprised of an HLHS proband and four family members who underwent echocardiography and whole-genome sequencing (WGS). Dermal fibroblast-derived induced pluripotent stem cells (iPSC) were procured from the proband–parent trio and bioengineered into cardiomyocytes. Cardiac phenotyping revealed aortic valve atresia and a slit-like left ventricular cavity in the HLHS proband, isolated bicuspid pulmonary valve in his mother, BAV in a maternal 4° relative, and no CHD in his father or sister. Filtering of WGS for rare, functional variants that segregated with CHD and were compound heterozygous in

the HLHS proband identified *NOTCH1* as the sole candidate gene. An unreported missense mutation (P1964L) in the cytoplasmic domain, segregating with semilunar valve malformation, was maternally inherited and a rare missense mutation (P1256L) in the extracellular domain, clinically silent in the heterozygous state, was paternally inherited. Patient-specific iPSCs exhibited diminished transcript levels of *NOTCH1* signaling pathway components, impaired myocardiogenesis, and a higher prevalence of heterogeneous myofilament organization. Extended, phenotypically characterized families enable WGS-derived variant filtering for plausible Mendelian modes of inheritance, a powerful strategy to discover molecular underpinnings of CHD. Identification of compound heterozygous *NOTCH1* mutations and iPSC-based functional modeling implicate mutant allele burden and impaired myogenic potential as mechanisms for HLHS.

✉ Timothy M. Olson  
olson.timothy@mayo.edu

- <sup>1</sup> Cardiovascular Genetics Research Laboratory, Mayo Clinic, 200 First Street SW, Rochester, MN 55905, USA
- <sup>2</sup> Division of Pediatric Cardiology, Department of Pediatric and Adolescent Medicine, Mayo Clinic, Rochester, MN, USA
- <sup>3</sup> Division of Cardiovascular Diseases, Department of Internal Medicine, Mayo Clinic, Rochester, MN, USA
- <sup>4</sup> Division of General Internal Medicine, Department of Internal Medicine, Mayo Clinic, Rochester, MN, USA
- <sup>5</sup> Center for Regenerative Medicine, Mayo Clinic, Rochester, MN, USA
- <sup>6</sup> Division of Biomedical Statistics and Informatics, Department of Health Sciences Research, Mayo Clinic, Rochester, MN, USA

## Introduction

The molecular basis of hypoplastic left heart syndrome (HLHS) is poorly understood. Characterized by an underdeveloped left ventricle, aortic and mitral valves, and aorta, children born with this severe congenital heart defect (CHD) require staged, single ventricle surgical palliation or cardiac transplantation for survival. The fundamental principle of blood flow-induced fetal cardiac growth suggests that HLHS could be caused by developmental arrest of myogenesis, valvulogenesis, and/or vasculogenesis. Although HLHS typically occurs as a sporadic, apparently non-Mendelian disorder, genetic underpinnings of HLHS are implicated by recurrence risks of 2–4 % in families with one affected child and 25 % in families with two affected children (Norwood et al. 1983). Furthermore, screening

echocardiography in first-degree relatives has identified less severe, often asymptomatic CHD including bicuspid/stenotic aortic valve, hypoplastic aortic arch, and coarctation of the aorta (Loffredo et al. 2004; Wessels et al. 2005; McBride et al. 2005). Heterozygous *NOTCH1* mutations have in fact been identified in patients with a spectrum of left-sided cardiac malformations, including HLHS (Garg et al. 2005; Mohamed et al. 2006; McKellar et al. 2007; McBride et al. 2008; Iascone et al. 2012; Foffa et al. 2014). Functional characterization of mutant Notch1 (G661S and A683T) in mouse fibroblasts did not demonstrate altered protein expression, but both mutations reduced ligand-induced signaling (McBride et al. 2008) and ultimately impaired the efficiency of epithelial to mesenchymal cell transition (EMT) (Riley et al. 2011). Incomplete penetrance of *NOTCH1* missense mutations with extreme variability of intra- and inter-familial phenotypic expression implicates unknown genetic or environmental modifiers (Garg et al. 2005; McBride et al. 2008).

Here, we utilized whole-genome sequencing (WGS) for disease gene discovery in an extended, phenotypically characterized family comprised of a proband with HLHS and 1° and 4° relatives with semilunar valve malformations. This approach enabled inheritance-based filtering for rare, functional variants and revealed compound heterozygosity as an explanation for CHD severity. Procurement of induced pluripotent stem cells (iPSC) from the proband–parent trio provided for the first time a patient-specific cellular model of genetically defined HLHS, revealing impaired myogenic potential.

## Methods

### Study subjects

Five family members, including the proband with HLHS, provided written informed consent under a research protocol approved by the Mayo Clinic Institutional Review Board. Cardiac anatomy was assessed by two-dimensional echocardiography in all family members. Genomic deoxyribonucleic acid (DNA) was isolated from peripheral-blood white cells or saliva for all five family members and dermal fibroblasts were procured from the proband–parent trio.

### Genomic and bioinformatics analyses

Array comparative genomic hybridization using a custom 180 K oligonucleotide microarray (Agilent, Santa Clara, CA) was performed on DNA from the proband with a genome-wide functional resolution of approximately 100 kilobases. Deletions larger than 200 kilobases and duplications larger than 500 kilobases were considered clinically

relevant. WGS of DNA and variant call annotation were performed utilizing the Mayo Clinic Medical Genome Facility and Bioinformatics Core. Paired-end libraries were prepared using the TruSeq DNA v2 sample prep kit following the manufacturer's protocol (Illumina, San Diego, CA). Each whole-genome library was loaded into four lanes of a flow cell and 101 base pair paired-end sequencing was carried out on Illumina's HiSeq 2000 platform using TruSeq SBS sequencing kit version 3 and HiSeq data collection version 1.4.8 software. Reads were aligned to the hg19 reference genome using Novoalign version 2.08 (<http://novocraft.com>) and duplicate reads were marked using Picard (<http://picard.sourceforge.net>). Local realignment of insertion/deletions (INDELs) and base quality score recalibration were then performed using the Genome Analysis Toolkit version 1.6-9 (GATK) (McKenna et al. 2010). Single-nucleotide variants (SNV) and INDELs were called across all samples simultaneously using GATK's Unified Genotyper with variant quality score recalibration (DePristo et al. 2011).

Variant call format files with SNV and INDEL calls from each individual were uploaded and analyzed using Ingenuity® Variant Analysis™ software (QIAGEN, Redwood City, CA, USA) where variants were functionally annotated and filtered by an iterative process. First, a filter was put into place to select for rare, high-quality heterozygous variants that (a) had a read depth of at least 10; (b) were not adjacent to a homopolymer exceeding 5 base pairs; (c) were present in <5 whole-exome sequencing (WES) datasets collected from 147 individuals not affected with HLHS; (d) were not identified within the top 1 % most exonically variable genes; and (e) were present at a frequency <1 % in the Exome Variant Server (WES data from 6503 individuals) (Exome Variant Server 2014) and/or 1000 Genomes (WGS data from 1092 individuals) (The 1000 Genomes Consortium 2012). Functional variants were defined as those that impacted a protein sequence, canonical splice site, micro-RNA coding sequence/binding site, enhancer region, or transcription factor binding site within a promoter validated by ENCODE chromatin immunoprecipitation experiments (Raney et al. 2014). Using WGS data from five family members, rare functional variants were then filtered for (a) segregation with CHD and (b) compound heterozygosity in the HLHS proband.

### Linkage analysis

All five family members underwent genotyping and locus mapping using the Omni1 (I.1, I.2, II.1 and II.2) or Omni 2.5 (I.3) SNV chip. The average call rate for SNVs and individuals was greater than 98 %. A total of 593,743 SNVs overlapped between genotyping chips and had a call rate over 95 % with a minor allele frequency (MAF)

among the genotyped individuals above 5 %. Genomic positions from Rutgers were incorporated into the data for linkage analysis (Matisse et al. 2007). The number of SNVs was reduced to 13,991 when imposing the following criteria: MAF greater than 20 %, Hardy–Weinberg  $P > 10^{-5}$ , and pairwise  $r^2 < 0.05$ . Population allele frequencies for linkage analysis were retrieved from the CEU population in the November 23, 2010 release of the 1000 genomes data (The 1000 Genomes Consortium 2012). Data were prepared using SAS (version 9.3, SAS Institute, Cary, NC), R (version 3.0.2, R Foundation for Statistical Computing, Vienna, Austria), PLINK (version 1.07) and VCFTools (version 0.1.7) (Purcell et al. 2007; Danacek et al. 2011). Parametric linkage analyses were performed with Merlin (Version 1.1.2) (Abecasis et al. 2002), modeling dominant inheritance and specifying the following variables: phenocopy rate 0.005, dichotomous liability classes ('affected' and 'unaffected') and a 100 % penetrance model.

### iPSC and patient-specific cardiomyocyte analysis

**Cell culture** Reprogrammed iPSCs (ReGen Theranostics, Rochester, MN) from the proband–parent trio were maintained on mouse embryonic fibroblasts in DMEM/F12 supplemented with 20 % KOSR, recombinant human FGF basic (20 ng/ml; R&D Systems, Minneapolis, MN), non-essential amino acids (EMD Millipore, Billerica, MA), L-glutamax, and 2-mercaptoethanol (Sigma, St. Louis, MO). Unless specified otherwise, cell culture reagents were purchased from Invitrogen (Carlsbad, CA). For comparison of mRNA transcript levels in iPSCs, all clones were adapted to mTeSR (StemCell Technologies, Vancouver, British Columbia) prior to sample collection. To differentiate iPSCs into the cardiac lineage, cells were cultured for one passage on Geltrex (LDEV-Free, hESC-qualified, reduced growth factor) in MEF-conditioned medium (iPSC maintenance medium conditioned for 24 h by MEFs) for depletion of feeder cells, then dissociated using TrypLE Select and plated as a monolayer. At confluence, the medium was changed to RPMI supplemented with B27 (minus insulin), which served as the maintenance medium for differentiating cells. For days 0–4 of cardiac differentiation, Activin A (10 ng/ml; R&D Systems) and BMP4 (20 ng/ml; R&D Systems) were included in the medium. To obtain cardiomyocytes from the proband's iPSCs for myofilament analysis, medium was supplemented with Activin A (100 ng/ml) for the first 24 h, and for days 1–5 the differentiation medium included BMP4 (10 ng/ml) and FGF basic (5 ng/ml). The differentiating cells were maintained in 5 % oxygen for days 0–14. All iPSC-derived cardiomyocytes were transferred to coverslips at day 30 and harvested at day 50.

**Gene expression** Total RNA was extracted with TRIzol Reagent (Invitrogen) and purified using a Qiagen RNeasy Mini Kit. cDNA synthesis was completed using reagents supplied in the iScript cDNA Synthesis Kit (Bio-Rad Laboratories, Hercules, CA).

qPCR reactions consisted of cDNA, TaqMan Universal PCR Master Mix (Life Technologies, Carlsbad, CA), and PrimeTime predesigned assay primers (Integrated DNA Technologies, Inc., Coralville, IA), and were completed using an Applied Biosystems 7500 Real-Time PCR System. Primer sets included *HES1* (Hs.PT.56a.4181121), *HEY1* (Hs.PT.56a.4299267.g), *NOTCH1*-intracellular domain (Hs.PT.58.39600723), and *GAPDH* (Hs.PT.39a.22214836).

**Immunofluorescent staining** iPSCs and iPSC cardiomyocytes were fixed with 4 % paraformaldehyde (Sigma), permeabilized with 0.5 % Tween20 (Sigma) and blocked overnight with SuperBlock Blocking Buffer. Primary antibodies included Sox2 (EMD Millipore), SSEA3 (Stemgent, Cambridge, MA), and Tra-1-60 (EMD Millipore) for iPSCs, and  $\alpha$ -actinin (clone EA-53; Sigma) and sarcomeric myosin heavy chain (MF20) (Developmental Studies Hybridoma Bank, Iowa City, IA) for iPSC cardiomyocytes. Secondary antibodies were conjugated with an Alexa Fluor<sup>®</sup> 488, 568, or 633 dye. Samples were mounted with ProLong<sup>®</sup> antifade reagent with DAPI. Images were acquired on a Zeiss LSM 510 Meta confocal microscope.

**Flow cytometry** Differentiating iPSCs were dissociated into a single cell suspension by treatment with Worthington Biochemical Type 2 Collagenase II followed by 0.05 % Gibco<sup>®</sup> Trypsin–EDTA, and then exposed to the LIVE/DEAD<sup>®</sup> Fixable Near-IR Dead Cell Stain. Cells were fixed and permeabilized using IntraPrep (Beckman Coulter, Indianapolis, IN) and stained with MF20 Alexa Fluor<sup>®</sup> 488 (eBioscience, San Diego, CA). Data were collected with a Gallios flow cytometer (Beckman Coulter) and analyzed with Kaluza 1.2.

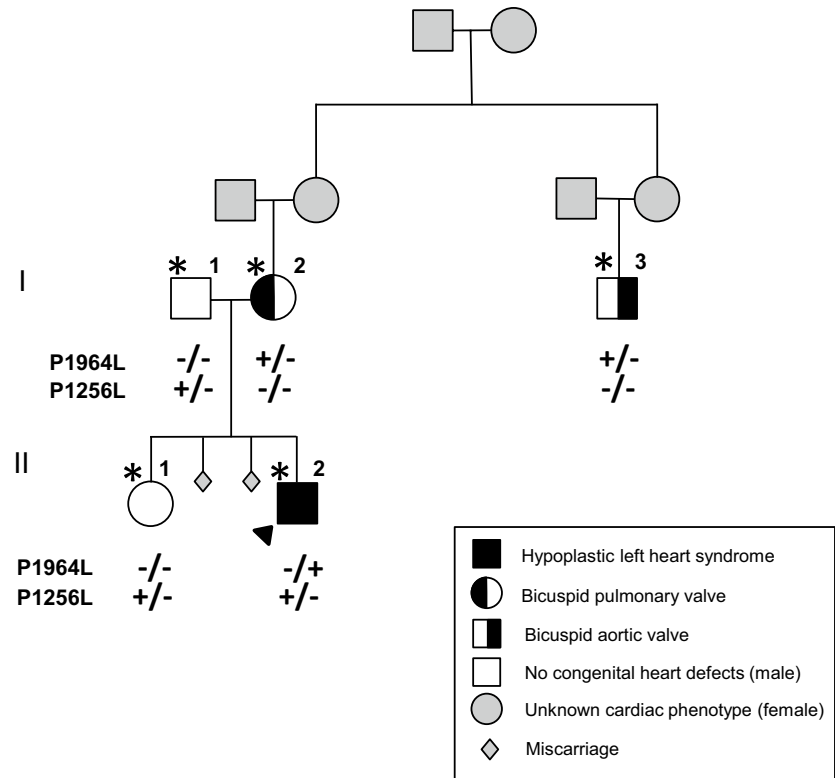
**Statistics** Data are presented as the mean  $\pm$  SEM. Significant differences were calculated with a two-tailed Student's *t* test with Welch's correction when appropriate using Prism5 (Graphpad Software, La Jolla, CA). A  $P < 0.05$  was considered significant.

## Results

### Family phenotype

We identified and phenotypically characterized a family of White European ancestry, comprised of three individuals with CHD of varying severity (Fig. 1). On the first day of life, the proband (II.2) was diagnosed with HLHS with severe mitral stenosis, aortic valve atresia, slit-like left ventricular cavity, and hypoplastic ascending aorta (4 mm

**Fig. 1** Pedigree of family with variably expressed congenital heart disease. Genotypes indicate presence (+) or absence (–) of the *NOTCH1*-P1256L and/or *NOTCH1*-P1964L amino acid substitution. The proband, with the severe CHD phenotype of HLHS, was compound heterozygous for these mutations. A filled triangle designates the proband whereas an asterisk (\*) indicates family members who underwent whole-genome sequencing



diameter). He had no apparent extra-cardiac abnormalities. His 1° family members underwent screening echocardiography for our research study. His mother (I.2) was asymptomatic with a bicuspid pulmonary valve (BPV) and his father (I.1) and sister (II.1) had no CHD. Family history and medical records review revealed a 4° maternal relative (I.3) previously diagnosed with BAV at age 32, who underwent aortic valve replacement at age 41 for progressive calcific aortic valve stenosis. Maternal history was notable for two prior miscarriages at 8 and 11 weeks gestation.

### Whole-genome sequencing and bioinformatics analysis

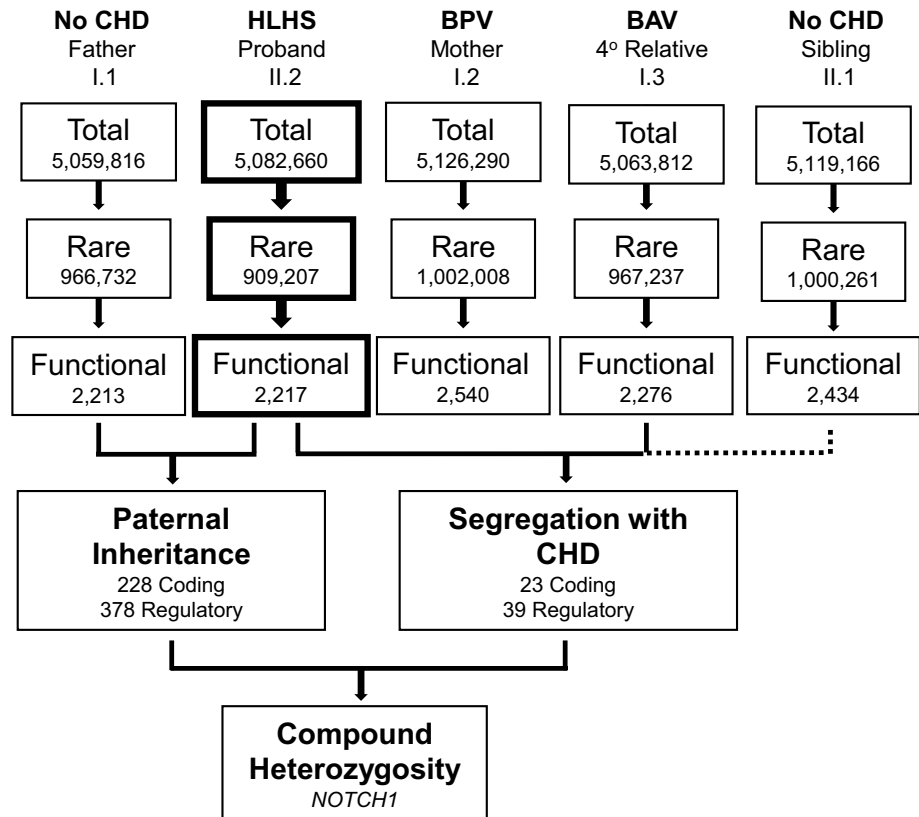
Array comparative genomic hybridization analysis excluded aneuploidy in the HLHS proband. To identify pathogenic coding or regulatory SNVs or INDELs, WGS was carried out on all five family members. Each sample yielded approximately 1.5 billion 101 base paired-end reads which passed quality control standards with 95 % of the reads mapping to the genome. After marking and filtering out duplicate reads, over 99 % of the hg19 human reference genome had coverage. The average depth across the genome was 42X and an average of 95 % of the gene body regions (exons, introns, and 5' and 3' untranslated regions) demonstrated a minimal read depth of 20 reads. Each family member had approximately 5 million variants which, upon filtering for rarity, function and mode of inheritance, were reduced to two missense mutations in the

HLHS proband (Fig. 2). Both mutations were identified in *NOTCH1*, encoding neurogenic locus notch homolog protein 1. The mutation on the paternal allele localized to extracellular EGF-like domain 32 (exon 23: c.3767 C > T, p.P1256L), while the mutation on the maternal allele localized to the intracellular ankyrin 2 domain (exon 31: c.5891 C > T, p.P1964L) (Fig. 3a). *NOTCH1* has a residual variant intolerance score of 0.33 %, indicating its tolerance of genetic variation is less than 99 % of other genes (Petrovski et al. 2013), and the altered amino acid residues are highly conserved across species (Fig. 3b). *NOTCH1*-P1964L, an unreported mutation that segregated with variably expressed CHD, was predicted to be damaging by both SIFT (Ng and Henikoff 2001) and Polyphen2 (Adzhubei et al. 2010). *NOTCH1*-P1256L was also identified in the unaffected father and sibling and, while predicted to be benign by SIFT (Ng and Henikoff 2001) and Polyphen2 (Adzhubei et al. 2010) is extremely rare in 28,800 ethnically matched, unrelated European (Non-Finnish) individuals who comprise the Exome Aggregation Consortium (ExAC) database (allele frequency = 0.000048) (Fig. 3c) (Exome Aggregation Consortium 2015).

### Linkage analysis

To validate our findings and ensure that mutations in equally plausible candidate genes were not missed by poor WGS coverage, we performed linkage analysis

**Fig. 2** Whole-genome sequencing data filtering scheme. An iterative filtering approach was applied to single nucleotide and insertion/deletion variants identified in each family member. Rarity and functional impact of the variant were used as inclusion criteria. Postulating that mutant allele burden accounted for severity of the congenital heart defect, variants were subsequently filtered for compound heterozygosity in the proband, whereby the maternal variant segregated with CHD. Paternally and maternally inherited missense mutations in *NOTCH1* were the only variants that fulfilled filtering criteria. The dashed line indicates a subtractive filter for the unaffected sibling. *HLHS* hypoplastic left heart syndrome, *CHD* congenital heart defect, *BPV* bicuspid pulmonary valve, *BAV* bicuspid aortic valve



recognizing that the family was underpowered for conclusive locus mapping. We identified seven equally plausible loci (peak LOD scores of 1.1) based on haplotypes shared by the three family members with CHD but not the proband's unaffected sibling. The five loci spanned 1421 genes, one of which was *NOTCH1*. The candidacy of all 1421 genes was assessed based on an established association with CHD, utilizing the Ingenuity® Variant Analysis™ software Knowledge Base, a manually curated resource that integrates data from top-tier scientific literature. In addition to *NOTCH1*, there were 25 other genes associated with CHD. However, none of these genes harbored a rare functional mutation. Visual inspection of the raw data utilizing the Integrated Genomics Viewer (Robinson et al. 2011) revealed ample coverage of each gene, verifying that the segregating *NOTCH1* mutation was the sole candidate.

### In vitro modeling

Dermal samples were collected from the father, mother, and proband and fibroblast outgrowths were expanded in culture for a brief period prior to reprogramming with a cocktail of lentiviruses carrying POU5F/OCT4, SOX2, KLF4, or c-MYC. After a period of approximately 3 weeks, colonies with morphology similar to

human embryonic stem cells (hESCs) were selected and expanded. Each established clone was characterized by immunofluorescent staining for standard pluripotency markers including SSEA-3, Tra-1-60, and Sox2 (Fig. 4a), as well as Oct4 and Nanog (data not shown), yielding three clones for the proband, three clones for the mother and two clones for the father which underwent further experimentation. Because it has been reported that several Notch signaling pathway components are expressed in hESCs (Yu et al. 2008), the mRNA transcript levels for *NOTCH1* and its downstream targets *HES1* and *HEY1* were measured by RT-qPCR. The expression levels of these components were similar among the clones established for both parents. In contrast, the levels of these components were approximately twofold lower in the proband compared to parents (*NOTCH1*  $P = 0.005$ , *HES1*  $P = 0.008$ , and *HEY1*,  $P = 0.007$ ) (Fig. 4b). These data indicate that the Notch signaling pathway is dysregulated in the proband's iPSCs. Next, all iPSC clones were differentiated into the cardiovascular lineages starting from a monolayer of cells and using an adaptive protocol that combines Activin A and BMP4 in RPMI-based differentiation medium for the first 4 days, followed by maintenance in unmodified differentiation medium (Fig. 4c). By day 16, robust areas of beating were observed in the iPSC clones from the parents, and small beating clusters

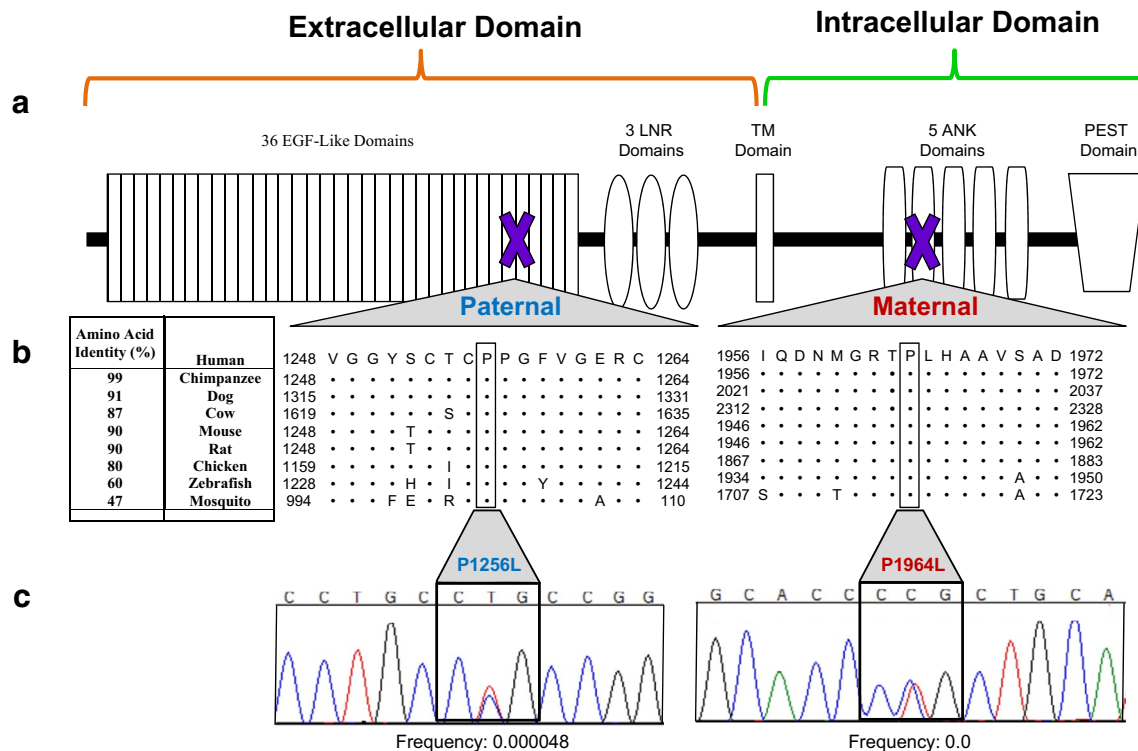


**Fig. 3** Location and conservation of *NOTCH1* mutations. **a** The protein topology is shown, with location of maternal and paternal mutations indicated by a purple “X”. **b** Amino acid identities of full-length *NOTCH1* protein in other species compared to humans is indicated. In addition, conservation of each region that contains the mutated

residue (boxed) is shown, whereby filled circle indicates identical residues. **c** The identified *NOTCH1* mutations, verified by Sanger sequencing, were rare (P1256L) or unreported (P1964L) in 28,800 European (Non-Finnish) individuals in the ExAC database

were observed with the iPSC clones from the proband. At day 20, the differentiated cells were dissociated into a single cell suspension and analyzed by flow cytometry to determine the percentage of cardiomyocytes within the cell population based on the expression of MF20. On average, 65 % of the cells were MF20+ in the iPSC clones for the parents, whereas only 17 % of the cells were MF20+ with the iPSC clones from the proband ( $P < 0.0001$ ) (Fig. 4d). For a final assessment, the myofibril organization of d50 iPSC cardiomyocytes was examined by immunocytochemistry for the sarcomeric protein  $\alpha$ -actinin. In comparison to the iPSC-derived cardiomyocytes obtained from the parents ( $n = 195$ ), those obtained from the proband’s iPSCs ( $n = 208$ ) had a higher percentage of cells (42 vs. 11 %) in which sarcomeric  $\alpha$ -actinin exhibited either a punctate staining pattern or short fragmented myofibrils in greater than one-fourth of the total cellular area ( $P = 0.03$ ) (Fig. 4e). However, no differences were observed in the size of the iPSC cardiomyocytes, which is similar to what has been reported for iPSCs from patients with dilated cardiomyopathy (Sun et al. 2012).

## Discussion

### Role of *NOTCH1* in cardiac development

*NOTCH1*, encoding neurogenic locus notch homolog protein 1, is a single-pass transmembrane receptor in the evolutionarily conserved Notch signaling pathway that has been shown to play a vital role in murine cardiac development (High and Epstein 2008). Activation results in its cleavage and nuclear translocation of the intracellular domain to guide transcription of downstream targets, which are required during multiple phases of cardiogenesis. During ventricular morphogenesis, elevated expression of *Notch1* in the developing trabeculae is critical for differentiation of cardiomyocytes and proper development of the ventricular chambers (Grego-Bessa et al. 2007). *Notch1* is also necessary for cardiac valvulogenesis due to its role in EMT, a transformation of cells required for proper development of cardiac valves (Timmerman et al. 2004). Mice lacking functional protein due to a targeted homozygous *Notch1* mutation die at embryonic day 10.5 (Swiatek et al. 1994) with a collapsed endocardium and paucity of mesenchymal

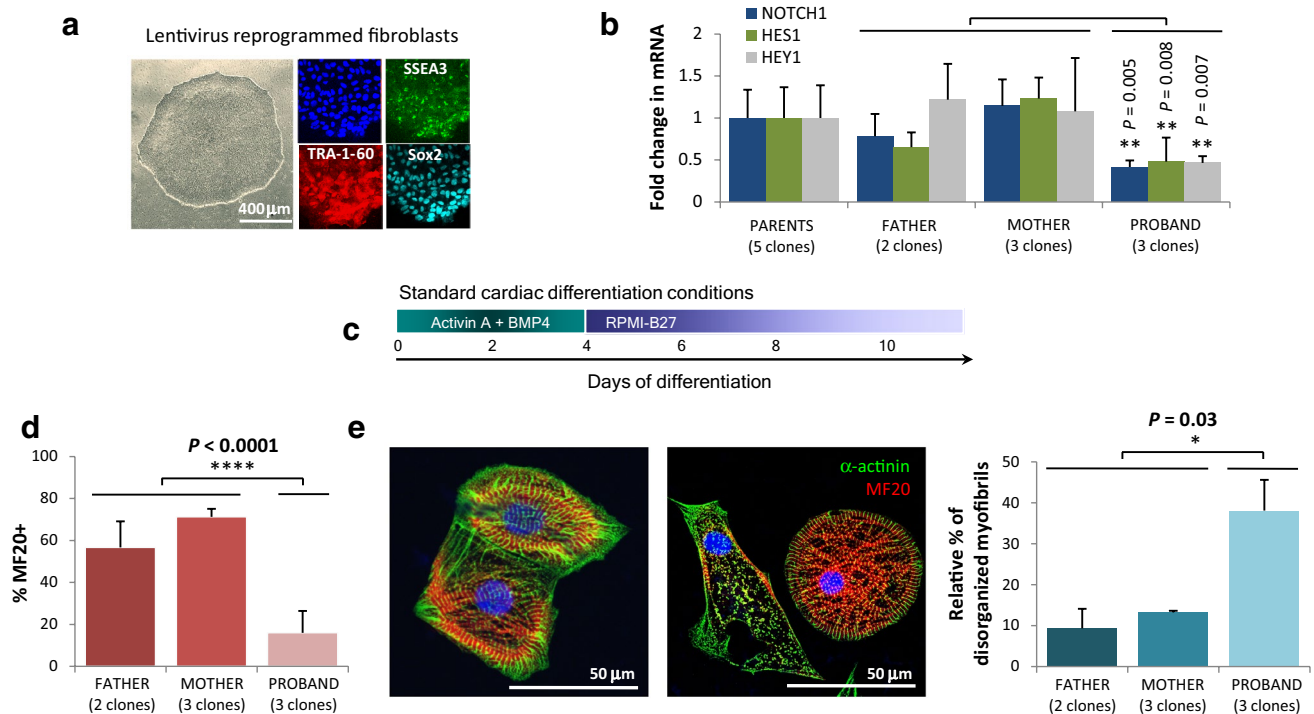


**Fig. 4** Patient-specific induced pluripotent stem cells model impaired cardiogenesis. **a** Morphology and immunostaining of induced pluripotent stem cells (iPSCs) with pluripotency markers (SSEA3, *green*; TRA-1-60, *red*; Sox2, *cyan*; DAPI, *blue*). **b** Quantitative reverse-transcription PCR was performed in three unique clones from the HLHS proband and normalized to the levels measured for both parents (two clones from the father and three clones from the mother). A statistically significant difference (\*\*) in levels of *NOTCH1*, *HES1* and *HEY1* ( $P = 0.005$ ,  $P = 0.008$ , and  $P = 0.007$ , respectively) were observed in the proband. **c** Differentiation approach to induce in vitro cardiogenesis utilizing an adaptive Activin A/BMP4 tailored to clonal

variations. **d** Quantification of cardiomyocyte yield by flow cytometry after 20 days of differentiation demonstrates decreased cardiogenesis in the HLHS proband ( $P < 0.0001$ ). **e** Immunofluorescent staining of d50 iPSC cardiomyocytes for  $\alpha$ -actinin (AF488) and sarcomeric myosin heavy chain/MF20 (AF568) for the father (*left*) and proband (*right*). Scale bar is 50  $\mu$ m. Compared to iPSC cardiomyocytes from both parents ( $n = 195$ ), iPSC cardiomyocytes from the proband ( $n = 208$ ) show a punctate sarcomeric  $\alpha$ -actinin or cardiac troponin T staining pattern in greater than one-fourth of the total cellular area or abnormal sarcomeric organization of myofibrils ( $P = 0.03$ , two-tailed Student's *t* test)

cushion cells due to severe impairment of EMT (Timmerman et al. 2004). The association of *NOTCH1* with valvulogenesis was also observed in zebrafish where its constitutive activation lead to hypercellular cardiac valves (Timmerman et al. 2004).

### Heterozygous *NOTCH1* mutations in CHD

*NOTCH1* mutations associated with abnormal cardiac development were first identified by genome-wide locus mapping and mutation scanning in two families with a spectrum of autosomal dominant CHDs including BAV, ventricular septal defect, tetralogy of Fallot, mitral stenosis, and mitral atresia with left ventricular hypoplasia and double outlet right ventricle (Garg et al. 2005). Within each family, identification of a heterozygous nonsense or frameshift mutation resulted in a truncated *NOTCH1* transcript. Subsequent candidate gene studies identified thirteen heterozygous mutations in *NOTCH1* in individuals with BAV (Mohamed et al. 2006; McKellar et al. 2007; McBride et al. 2008; Foffa et al.

2014), aortic valve stenosis (McBride et al. 2008), coarctation of the aorta (McBride et al. 2008), or HLHS (McBride et al. 2008; Iascone et al. 2012). Ten were missense mutations (eight extracellular, two cytoplasmic), all reported at low frequencies in ~60,000 individuals who make up the ExAC database (allele frequencies = 0.000008–0.013), supporting their role as CHD susceptibility alleles with variable expressivity. In contrast, three were unreported loss of function mutations, including an inherited nonsense mutation in two family members with BAV (Foffa et al. 2014) and de novo frameshift and splice site mutations in two unrelated probands with HLHS (Iascone et al. 2012). Functional characterization of two of the missense mutations, each linked to diverse CHDs and reported in ExAC (A683T = 0.0028 and G661S = 0.038), demonstrated impaired EMT due to perturbed downstream Notch1 signaling (Riley et al. 2011). To our knowledge, genetic or environmental factors that modify phenotypic expression of *NOTCH1* mutations and account for the severe HLHS phenotype have not been identified previously.

## Compound heterozygous *NOTCH1* mutations and impaired myogenic potential in HLHS

Using WGS and a family-based variant filtering approach, we demonstrate for the first time compound heterozygous *NOTCH1* mutations in a patient with HLHS. Our strategy enabled a comprehensive survey of essentially all genes with no a priori assumptions of gene candidates or disease mechanisms. While advances are being made in elucidating the complex genetics of CHD, complete understanding of its genetic underpinnings remains a challenge due, in part, to modifier genes/mutations. WGS is now able to provide all of the unique variants in a personal genome, but pinpointing those which are involved in the pathogenesis of CHD is not a simple task (Gelb and Chung. 2014). Here, we capitalized on maternal segregation of variably expressed CHD, using the unaffected sibling as a subtractive filter, and specified compound heterozygosity in the HLHS proband as a plausible inheritance model. This provided robust evidence for *NOTCH1* as the top candidate, without imposing filters based on imprecise in silico predictions of a variant's biological significance. The unreported P1964L mutation on the maternal allele segregated with BPV and BAV in other family members and is the first identified CHD-associated *NOTCH1* mutation to reside within the intracellular ankyrin repeat domain, disrupting a highly conserved consensus motif in the first helix of ankyrin repeat 2 (Ehebauer et al. 2005). To our knowledge, it is also the first *NOTCH1* mutation associated with pulmonary valve malformation, implicating a role of NOTCH1 signaling in right heart development. The P1256L mutation on the paternal allele is rare but clinically silent in the father and sibling. This is consistent with other CHD-associated *NOTCH1* missense mutations that are present in control databases and variably penetrant (Mohamed et al. 2006; McKellar et al. 2007; McBride et al. 2008; Foffa et al. 2014). Our genetic data suggested a genotype–phenotype relationship whereby mutant allele burden may determine the degree of NOTCH1 signaling impairment and corresponding severity of phenotypic expression. We speculate that synergistic heterozygosity for mutations in different NOTCH1 signaling protein genes could underlie other cases of HLHS.

To validate that the identified compound heterozygous *NOTCH1* mutations could significantly contribute to HLHS, an in vitro platform was created to screen the cardiogenicity of patient-specific iPSCs and examine the myofilament organization of the iPSC-derived cardiomyocytes for disease-susceptibility characteristics. Comparison of *NOTCH1* transcript levels and two of its primary effectors in iPSCs bioengineered from the proband and parents indicated that the Notch signaling pathway was dysregulated in the proband. As a consequence, the iPSC-derived cardiomyocyte yield was diminished in conditions that supported cardiomyogenesis. Moreover, in vitro culture of

the iPSC cardiomyocytes from the HLHS proband led to increased sarcomeric disorganization and myofibril disarray. While these data did not achieve statistical significance when comparing the mother and father, it is plausible that a single heterozygous mutation in *NOTCH1* confers subtle changes in its expression and activity that require more sensitive assays and/or additional clones. Our findings are consistent with two previous studies that have reported reduced cardiomyocyte yields and a higher prevalence of myofibril disorganization in iPSCs derived from patients with HLHS compared to unrelated controls (Jiang et al. 2014; Kobayashi et al. 2014). Uniquely, our study is the first to model genetically defined HLHS with iPSC-derived cardiomyocytes using parental cells as controls, providing further evidence for impaired myogenic potential as a mechanism for HLHS.

**Acknowledgments** The authors gratefully acknowledge the patients and family members who participated in this study.

### Compliance with ethical standards

**Informed consent** Informed consent was obtained from all individual participants included in the study.

**Funding** Todd and Karen Wanek Family Program for Hypoplastic Left Heart Syndrome, Mayo Clinic Foundation.

**Conflict of interest** Mayo Clinic and Timothy J. Nelson have a Financial Conflict of Interest managed according to established policies in the context of licensed technology to ReGen Theranostics, Inc.

## References

- Abecasis GR, Cherny SS, Cookson WO, Cardon LR (2002) Merlin-rapid analysis of dense genetic maps using sparse gene flow trees. *Nat Genet* 30:97–101. doi:10.1038/ng786
- Adzhubei IA, Schmidt S, Peshkin L, Remensky VE, Gerasimova A, Bork P, Kondrashov AS, Sunyaev SR (2010) A method and server for predicting damaging missense mutations. *Nat Method* 7:248–249. doi:10.1038/nmeth0410-248
- Danacek P, Auton A, Abecasis G, Albers CA, Banks E, DePristo MA, Handsaker RE, Lunter G, Marth GT, Sherry ST, McVean G, Durbin R, 1000 Genomes Project Analysis Group (2011) The variant call format and VCF tools. *Bioinformatics* 27:2156–2158. doi:10.1093/bioinformatics/btr330
- DePristo MA, Banks E, Poplin RE, Garimella KV, Maguire JR, Hartl C, Philippakis AA, del Angel G, Rivas MA, Hanna M, McKenna A, Fennell TJ, Kernysky AM, Sivachenko AY, Cibulskis K, Gabriel SB, Altshuler D, Daly MJ (2011) A framework for variation discovery and genotyping using next-generation DNA sequencing data. *Nat Genet* 43:491–498. doi:10.1038/ng.806
- Ehebauer MT, Chirgadze DY, Hayward P, Martinez Arias A, Blundell TL (2005) High-resolution crystal structure of the human Notch 1 ankyrin domain. *Biochem J* 392:13–20. doi:10.1042/BJ20050515
- Exome Aggregation Consortium (ExAC), Cambridge, MA (2015). <http://exac.broadinstitute.org>
- Exome Variant Server (2014) NHLBI GO Exome Sequencing Project (ESP), Seattle, WA. <http://evs.gs.washington.edu/EVS>



- Foffa I, Ait Ali L, Panesi P, Mariani M, Festa P, Botto N, Vecoli C, Andreassi MG (2014) Sequencing of *NOTCH1*, *GATA5*, *TGFBR1* and *TGFBR2* genes in familial cases of bicuspid aortic valve. *BMC Med Genet* 16:1–9. doi:[10.1186/1471-2350-14-44](https://doi.org/10.1186/1471-2350-14-44)
- Garg V, Muth AN, Ransom JF, Schluterman MK, Barnes R, King IN, Grossfeld PD, Srivastava D (2005) Mutations in *NOTCH1* cause aortic valve disease. *Nature* 437:270–274. doi:[10.1038/nature03940](https://doi.org/10.1038/nature03940)
- Gelb BD, Chung WK (2014) Complex genetics and etiology of human congenital heart disease. *Cold Spring Harb Perspect Med* 4:1–12. doi:[10.1101/cshperspect.a013953](https://doi.org/10.1101/cshperspect.a013953)
- Grego-Bessa J, Luna-Zurita L, del Monte G, Bolos V, Melgar P, Arandilla A, Garratt AN, Zang H, Mukoyama Y, Chen H, Shou W, Ballestar E, Esteller M, Rojas A, Perez-Pomares JM, de la Pompa JL (2007) Notch signaling is essential for ventricular chamber development. *Dev Cell* 12:415–429. doi:[10.1016/j.devcel.2006.12.011](https://doi.org/10.1016/j.devcel.2006.12.011)
- High FA, Epstein JA (2008) The multifaceted role of Notch in cardiac development and disease. *Nature Rev* 9:49–61. doi:[10.1038/nrg2279](https://doi.org/10.1038/nrg2279)
- Iascone M, Ciccone R, Galletti L, Marchetti D, Seddio F, Lincesso AR, Pezzoli L, Vetro A, Barachetti D, Boni L, Federici D, Soto AM, Comas JV, Ferrazzi P, Zuffardi O (2012) Identification of de novo mutation and rare variants in hypoplastic left heart syndrome. *Clin Genet* 81:542–554. doi:[10.1111/j.1399-0004.2011.01674](https://doi.org/10.1111/j.1399-0004.2011.01674)
- Jiang Y, Habibollah S, Tilgner K, Collin J, Barta T, Al-Aama JY, Tesarov L, Hussain R, Trafford AW, Kirkwood G, Sernagor E, Eleftheriou CG, Przyborski S, Stojkovic M, Lako M, Keavney B, Armstrong L (2014) An induced pluripotent stem cell model of hypoplastic left heart syndrome reveals multiple expression and functional differences in HLHS-derived cardiac myocytes. *Stem Cells Transl Med* 3:416–423. doi:[10.5966/sctm.2013-0105](https://doi.org/10.5966/sctm.2013-0105)
- Kobayashi J, Yoshida M, Tarui S, Hirata M, Negai Y, Kasahara S, Naruse K, Ito H, Sano S, Oh H (2014) Directed differentiation of patient-specific induced pluripotent stem cells identifies the transcriptional repression and epigenetic modification of *NKX2-5*, *HAND1*, and *NOTCH1* in hypoplastic left heart syndrome. *PLoS One* 9:1–14. doi:[10.1371/journal.pone.0102796](https://doi.org/10.1371/journal.pone.0102796)
- Loffredo CA, Chokkalingam A, Sill AM, Boughman JA, Clark EB, Scheel J, Brenner JJ (2004) Prevalence of congenital cardiovascular malformations among relatives of infants with hypoplastic left heart, coarctation of the aorta, and d-transposition of the great arteries. *Am J Med Genet A* 124A:225–230. doi:[10.1002/ajmg.a.20366](https://doi.org/10.1002/ajmg.a.20366)
- Matise TC, Chen F, Chen W, De La Vega FM, Hansen M, He C, Hyland FCL, Kennedy GC, Kong X, Murray SS, Ziegler JS, Stewart WCL, Buyske S (2007) A second-generation combined linkage-physical map of the human genome. *Genome Res* 17:1783–1786. doi:[10.1101/gr.7156307](https://doi.org/10.1101/gr.7156307)
- McBride KL, Pignatelli R, Lewin M, Ho T, Fernbach S, Menesses A, Lam W, Leal SM, Kaplan N, Schliekelman P, Towbin JA, Belmont JW (2005) Inheritance analysis of congenital left ventricular outflow tract obstruction malformations: segregation, multiplex relative risk, and heritability. *Am J Med Genet A* 134A:180–186. doi:[10.1002/ajmg.a.30602](https://doi.org/10.1002/ajmg.a.30602)
- McBride KL, Riley MF, Zender GA, Fitzgerald-Butt SM, Towbin JA, Belmont JW, Cole SE (2008) *NOTCH1* mutations in individuals with left ventricular outflow tract malformations reduce ligand-induced signaling. *Hum Mol Genet* 17:2886–2893. doi:[10.1093/hmg/ddn187](https://doi.org/10.1093/hmg/ddn187)
- McKellar SH, Tester DJ, Yagubyan M, Majumdar R, Ackerman MJ, Sundt TM 3rd (2007) Novel *NOTCH1* mutations in patients with bicuspid aortic valve disease and thoracic aortic aneurysms. *J Thorac Cardiovasc Surg* 134:290–296. doi:[10.1016/j.jtcvs.2007.02.041](https://doi.org/10.1016/j.jtcvs.2007.02.041)
- McKenna A, Hanna M, Banks E, Sivachenko A, Cibulskis K, Kernysky A, Garimella K, Altshuler D, Gabriel S, Daly M, DePristo MA (2010) The genome analysis toolkit: a MapReduce framework for analyzing next-generation DNA sequencing data. *Genome Res* 20:1297–1303. doi:[10.1101/gr.107524.110](https://doi.org/10.1101/gr.107524.110)
- Mohamed SA, Aherrahrou Z, Liptau H, Erasmi AW, Hagemann C, Wrobel S, Borzym K, Schunkert H, Sievers HH, Erdmann J (2006) Novel missense mutations (p. T596M and p.P1797H) in *NOTCH1* in patients with bicuspid aortic valve. *Biochem Biophys Res Commun* 345:1460–1465. doi:[10.1016/j.bbrc.2006.05.046](https://doi.org/10.1016/j.bbrc.2006.05.046)
- Ng PC, Henikoff S (2001) Predicting deleterious amino acid substitutions. *Genome Res* 11:863–874. doi:[10.1101/gr.176601](https://doi.org/10.1101/gr.176601)
- Norwood WI, Lang P, Hansen DD (1983) Physiologic repair of aortic atresia-hypoplastic left heart syndrome. *N Engl J Med* 308:23–26. doi:[10.1056/NEJM198301063080106](https://doi.org/10.1056/NEJM198301063080106)
- Petrovski S, Wang Q, Heinzen EL, Allen AS, Goldstein DB (2013) Genic intolerance to functional variation and the interpretation of personal genomes. *PLoS Genet* 9:1–13. doi:[10.1371/journal.pgen.1003709](https://doi.org/10.1371/journal.pgen.1003709)
- Purcell S, Neale B, Todd-Brown K, Thomas L, Ferreira MAR, Bender D, Maller J, Sklar P, de Bakker PIW, Dal MJ, Sham PC (2007) PLINK: a tool set for whole-genome association and population-based linkage analysis. *Am J Hum Genet* 81:559–575. doi:[10.1086/519795](https://doi.org/10.1086/519795)
- Raney BJ, Dreszer TR, Barber GP, Clawson H, Fujita PA, Wang T, Nguyen N, Paten B, Zweig AS, Karolchik D, Kent WJ (2014) Track data hubs enable visualization of user-defined genome-wide annotations on the UCSC genome browser. *Bioinformatics* 30:1003–1005. doi:[10.1093/bioinformatics/btt637](https://doi.org/10.1093/bioinformatics/btt637)
- Riley MF, McBride KL, Cole SE (2011) *NOTCH1* missense alleles associated with left ventricular outflow tract defects exhibit impaired receptor processing and defective EMT. *Biochim Biophys Acta* 1812:121–129. doi:[10.1016/j.bbadis.2010.10.002](https://doi.org/10.1016/j.bbadis.2010.10.002)
- Robinson JT, Thorvaldsdottir Winckler W, Guttman M, Lander ES, Getz G, Mesirov JP (2011) Integrative genomics viewer. *Nat Biotechnol* 33:24–26. doi:[10.1038/nbt.1754](https://doi.org/10.1038/nbt.1754)
- Sun N, Yazawa M, Liu J, Han L, Sanchez-Freire V, Abilez OJ, Navarrete EG, Hu S, Wang L, Lee A, Pavlovic A, Lin S, Chen R, Hajjar RJ, Snyder MP, Dolmetsch RE, Butte MJ, Ashley EA, Longaker MT, Robbins RC, Wu JC (2012) Patient-specific induced pluripotent stem cells as a model for familial dilated cardiomyopathy. *Sci Transl Med* 4:130ra47. doi:[10.1126/scitranslmed.3003552](https://doi.org/10.1126/scitranslmed.3003552)
- Swiatek PJ, Lindsell CE, del Amo FF, Weinmaster G, Gridley T (1994) Notch1 is essential for postimplantation/development in mice. *Genes Dev* 8:707–719. doi:[10.1101/gad.8.6.707](https://doi.org/10.1101/gad.8.6.707)
- The 1000 Genomes Consortium (2012) An integrated map of genetic variation from 1092 human genomes. *Nature* 491:56–65. doi:[10.1038/nature11632](https://doi.org/10.1038/nature11632)
- Timmerman LA, Grego-Bessa J, Raya A, Bertran E, Perez-Pomares JM, Diez J, Aranda S, Palomo S, McCormick F, Izpisua-Belmonte JC, de la Pompa JL (2004) Notch promotes epithelial-mesenchymal transition during cardiac development and oncogenic transformation. *Genes Dev* 18:99–115. doi:[10.1101/gad.276304](https://doi.org/10.1101/gad.276304)
- Wessels MW, Berger RM, Frohn-Mulder IM, Roos-Hesselink JW, Hoogeboom JJ, Mancini GS, Bartelings MM, Krijger RD, Wladimiroff JW, Niermeijer MF, Grossfeld P, Willems PJ (2005) Autosomal dominant inheritance of left ventricular outflow tract obstruction. *Am J Med Genet A* 134A:171–179. doi:[10.1002/ajmg.a.30601](https://doi.org/10.1002/ajmg.a.30601)
- Yu X, Zou J, Ye Z, Hammond H, Chen G, Tokunaga A, Mali P, Li YM, Civin C, Gaiano N, Cheng L (2008) Notch signaling activation in human embryonic stem cells is required for embryonic, but not trophoblastic, lineage commitment. *Cell Stem Cell* 2:461–471. doi:[10.1016/j.stem.2008.03.001](https://doi.org/10.1016/j.stem.2008.03.001)